diffusion-fundamentals.org

The Open-Access Journal for the Basic Principles of Diffusion Theory, Experiment and Application

Beyond Fick: How Best to Deal with non-Fickian Behavior in a Fickian Spirit

John H. Petropoulos, Merope Sanopoulou and Kiki G. Papadokostaki

Inst. of Physical Chemistry, Demokritos National Research Center,
15310 Aghia Paraskevi, Athens, Greece

Corresponding author:
John H. Petropoulos
E-Mail: petrop@chem.demokritos.gr

Abstract

Starting from Fick's train of thought, which led to the formulation of his law governing diffusion in a solid or liquid medium, we first consider the limits of applicability of this law to solid medium-single penetrant systems. We then take up the question of proper formulation, in combination with simple but physically meaningful modeling, of diffusion behavior deviating from this law, because of (i) concentration dependence (ii) time dependence or (iii) space dependence, of the relevant transport parameters (which include the sorption, no less than the diffusion, coefficient). Examples of application to real systems are offered in each case. We conclude that progress in such studies depends on following Fick's mode of thinking rather than on adhering to the formalism of his law.

Keywords: Fick's law; Fickian diffusion; Non-Fickian diffusion; Diffusion in polymers; Diffusion in porous media; Permeation; Time-lag; Gas or vapor sorption; Case II diffusion; Viscoelastic swelling; Non-homogeneous media; Transport of matter.

1. Introduction: Formulation of Fick's law

Fundamental studies of the diffusion of penetrant micromolecules in solid media should fulfill two basic requirements:
(i) proper formulation of the diffusion process in terms of physically meaningful material parameters and
(ii) physical modeling of transport behavior under various conditions as a function of the physicochemical properties of the solid, the penetrant and the solid-penetrant system.

The geometry of the medium is not of prime importance in this respect. It is thus advantageous to use an experimental set up ensuring effectively unidimensional transport, such as diffusion across a sufficiently thin membrane or through a septum confined in a cylindrical holder.

The line of Fick's thinking on the subject of formulation may be described in his own words: "*It was quite natural to suppose that this law for the diffusion of a salt in its solvent must be identical with that, according to which the diffusion of heat in a conducting body takes place; upon this law Fourier founded his celebrated theory and it*

is the same which Ohm applied, with such extraordinary success, to the diffusion of electricity in a conductor"[1].

This seminal perception led Fick to the formulation of the flux density $J(x)$ of sorbed penetrant along the space coordinate $+x$, at any given time (t) and location (x) in the medium, as *proportional* to the corresponding concentration gradient $\partial C/\partial x$ (Fick's law). Thus, we have

$$J_x = -D(\partial C/\partial x) \tag{1}$$

where Fick's law requires *constant* diffusivity D. Clearly, this law was meant, (like its Fourier and Ohm counterparts) to apply to solid media exhibiting spatially uniform and time-independent properties not materially affected by the presence of sorbed penetrant. In fact, Fick's assignment to C the role of "diffusion potential", analogous to temperature or electrical potential, means *ipso facto* that C is presumed uniform across the membrane at equilibrium, i.e. $C(x,\ t\rightarrow\infty)=C_{eq}(x)$=const. Yet eq. (1) came subsequently to be regarded as a more or less general definition of diffusivity and was applied, sometimes indiscriminately (one might say in an unFickian way), to systems not conforming to the above restrictions, notably systems exhibiting transport properties, depending (a) on sorbed penetrant concentration C or (b) on the location x across the membrane or (c) on time t due to penetrant-induced microstructural relaxation of the medium. Pertinent examples are considered below.

2. Beyond Fick's Law: Irreversible Thermodynamic Approach

A more reasonable extension of Fick's law, worthy of Fick's original perceptive thinking, has been formulated by considering that diffusion occurs as a result of the disturbance of an equilibrium state characterized by uniformity of the chemical potential of the diffusing species μ (irrespective of the state of homogeneity or relaxation of the diffusion medium) [2]. Thus, it makes sense to assign to μ the role of diffusion potential and to regard sorbed molecules as moving (with macroscopic velocity u_x), under a driving force $\partial\mu/\partial x$, against the "frictional resistance" of the solid medium, measured by a frictional coefficient f_T (in complete analogy with the standard treatment of mechanical friction). Thus we may write

$$J_x = Cu_x = -(C/f_T)(\partial\mu/\partial x) = -(D_TC/RT)(\partial\mu/\partial x) \tag{2}$$

where the friction coefficient formalism has furthermore been transformed to an equivalent one, involving a "thermodynamic" diffusion coefficient (D_T), for easier comparison with D in eq. (1) (see e.g. [3, 4]). Eq. (2) may be rewritten in terms of the activity of sorbed penetrant a defined by

$$\mu = \mu^o + RT\ln a \tag{3}$$

where μ^o denotes a suitably chosen thermodynamic standard state. Eq. (2) then becomes

$$J_x = -D_TC(\partial\ln a/\partial x) = -D_TS(\partial a/\partial x) = -P(\partial a/\partial x) \tag{4}$$

where we have introduced the equilibrium parameter, known as the sorption coefficient, $S=(C/a)_{eq}$, and the permeability coefficient $P=D_TS$. The value of a, and hence of S, for

any given C, is determined in practice by equilibration with an external penetrant (e.g. gas or vapor) phase, where the activity of penetrant a_R, defined by

$$\mu_R = \mu_R^o + RT\ln a_R \tag{5}$$

is known. Then, if we choose $\mu^o = \mu_R^o$ (and given that $\mu=\mu_R$ at equilibrium), eqs (3) and (5) yield $a=a_R$.

Apart from a very substantial gain in generality, this "irreversible thermodynamic" (IRT) approach of eq. (4) also has the advantage of displaying explicitly the important role of the sorption coefficient S in diffusion processes.

3. Concentration-Dependent (Fickian) Diffusion

3.1 Theory

For systems characterized by a unique relation between C and a (known as the sorption isotherm), i.e. by S, which is either constant (Henry's law) or a function only of C or a, eq. (1) may be rewritten as

$$J_x = -D(\mathrm{d}C/\mathrm{d}a)(\partial a/\partial x) = -P(\partial a/\partial x) \tag{1a}$$

Comparison of eqs (1a) and (4) then yields a simple expression linking the Fick and thermodynamic diffusivities, namely (e.g. [3])

$$D \equiv D_T S(\mathrm{d}a/\mathrm{d}C) = D_T(\mathrm{d}\ln a/\mathrm{d}\ln C) = D_T\varphi_T \tag{6}$$

where φ_T is a "thermodynamic factor", the magnitude of which depends on the shape of the equilibrium sorption isotherm. In particular, we find $\varphi_T=1$ or $\varphi_T\neq1$ for solid-penetrant systems characterized by linear (S=const.) or nonlinear ($S\neq$const.) sorption isotherms, respectively and eq. (6) yields $D=D_T$ or $D\neq D_T$ respectively.

Thus, on the basis of the IRT approach:

(1) Fick's law ($D=D_T$=const.) also presupposes S=const. (thermodynamically ideal system).
(2) D as defined by Fick affords a proper measure of diffusivity only within the confines of Fick's law.
(3) Extension of Fick's formalism to cover non-ideal systems [$S=S(C)$], is thermodynamically acceptable, in view of the fact that the prerequisite $C(x, t\rightarrow\infty)\rightarrow C_{eq}(x)$ =const. (see above) is not violated (this is one good reason for calling such diffusion "Fickian") but compromises the significance of the resulting $D(C)$ as a physical kinetic parameter, to an extent depending on the behavior of φ_T in eq. (6).

Thus a non-ideal system may be formally characterized (as is done in standard texts, such as [5]) in terms of $D(C)$, determined by methods based on solutions of the classical diffusion equation

$$\partial C/\partial t = (\partial/\partial x)D(\partial C/\partial x) \tag{7}$$

which is obtained by substitution of eq. (1) in the mass conservation law

$$\partial C/\partial t = -\partial J/\partial x \tag{8}$$

However, it is important not to forgo the conversion of $D(C)$ to $D_I(C)$ via eq. (6) for a proper physical interpretation of diffusivity behavior, as illustrated in the example discussed in section 3.3 below.

3.2 Main experimental methods for the determination of diffusivity

Analytical (for D=const.) or numerical [for $D=D(C)$] solutions of eq. (7), are used in forms suitable for application to experimental work involving, most commonly, sorption or permeation experiments.

The typical experimental set up consists of a membrane of thickness l, the surfaces of which, at x=0, $x=l$, may be kept at chosen penetrant activities a_o, a_l respectively, by exposure to adjoining reservoirs (R1, R2) of pure penetrant (e.g. in the form of gas or vapor) maintained at the requisite gas or vapor pressures p_o, p_l, respectively (see Fig. 1a).

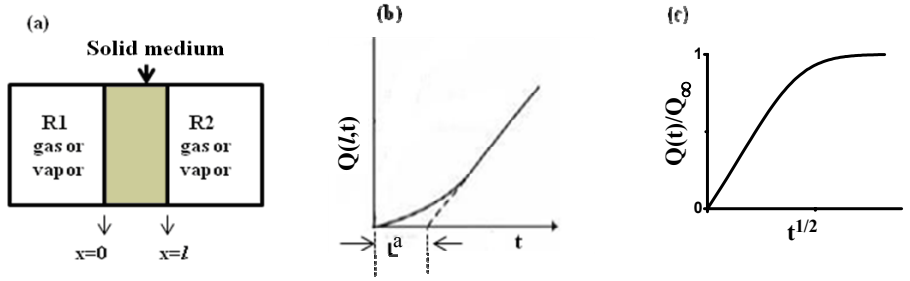

Fig. 1: Schematic representation of (a) experimental setup (b) typical permeation curve (c) typical (Fickian) absorption curve on a $t^{1/2}$ scale.

In a standard permeation experiment, the entire membrane is pre-equilibrated at a uniform activity $a=a_l$. The experiment is started, at time t=0, by instantaneously raising a at x=0 to $a=a_o>a_l$ and maintaining a_o and a_l constant thereafter, i.e.

$$a(x, t=0) = a_l\,; \quad a(x=0, t>0) = a_o = \text{const.}, \quad a(x=l, t>0) = a_l = \text{const.} \tag{9a,b,c}$$

One measures the quantity of penetrant (per unit membrane area), Q(l,t), which has entered the downstream reservoir (R2) at $x=l$, as a function of t, until a linear asymptote, $Q_S(l,t)$, is attained to an experimentally satisfactory degree of accuracy. The slope of this asymptote is the steady-state flux density J_S=const., while the intercept obtained by its back extrapolation to the t axis, is the time lag L^a (see Fig. 1b). We have

$$J_S = P_e(a_o - a_l)/l = D_e(C_o - C_l)/l \tag{10a,b}$$

where the experimental effective or integral permeabilities (P_e) and diffusivities (D_e) are defined on the basis of eqs (4) and (1) respectively and $C_o=Sa_o$, $C_l=Sa_l$; while

$$L^a = t - Q_S(l,t)/J_S \tag{11}$$

For systems obeying Fick's law:

$$P_e = P; \quad D_e = D; \quad L^a = l^2/6D \tag{12a,b,c}$$

Hence $S=P/D=6L^aP/l^2$ may be deduced purely from permeation data. For concentration-dependent systems P_e, D_e turn out to be arithmetic averages of $P(a_l \leq a \leq a_o)$ and $D(C_l \leq C \leq C_o)$ respectively, namely

$$P_e = \bar{P}(a_o, a_l) = (a_o - a_l)^{-1} \int_{a_l}^{a_o} P(a)da \tag{13a}$$

$$D_e = \bar{D}(C_o, C_l) = (C_o - C_l)^{-1} \int_{C_l}^{C_o} D(C)dC \tag{13b}$$

but there is no simple expression for L^a [5] permitting straightforward evaluation of D_e and of an effective sorption coefficient S_e, analogous to the case of S=const. Thus, knowledge of $S(C)$ from equilibrium sorption measurements is needed to evaluate $C_o=S(C_o)a_o$ and $C_l=S(C_l)a_l$, in order to deduce D_e from eq. (10b). Note, incidentally, that the assumption, sometimes made in the literature, that a meaningful S_e may be deduced from P_e/D_e, is erroneous. The only expression of this kind, which is valid for $C_l=a_l=0$, follows from eqs (10a,b) namely $S(C_o)=P_e/D_e$.

For a standard sorption experiment, the surface of the membrane at $x=l$ is blocked, the membrane is preequilibrated, as before, at uniform activity a_1 and the activity at $x=0$ is raised (absorption) or lowered (desorption) to a_o, which is maintained constant thereafter. The applicable boundary conditions are then:

$$a(x, t=0) = a_1\,; \quad a(x=0, t>0) = a_o = \text{const.}; \quad \partial a(x=l, t)/\partial x = 0 \tag{14a,b,c}$$

Alternatively, the membrane may remain in contact with both adjoining reservoirs and the activity changed from a_1 to a_o at $x=0$, l simultaneously, in which case eq. (14c) should be replaced by a condition analogous to (14b) for $x=l$, and the right hand side of eq. (15) below should be multiplied by 2.

One measures the quantity (per unit membrane area) of penetrant $Q(t)$ taken up (absorption) or released (desorption) by the membrane, as a function of time, up to final equilibrium $Q_\infty=l|C_o-C_1|=l|Sa_o-Sa_1|$ (see Fig. 1c). We have:

(a) At sufficiently short times (effective semi-infinite medium conditions) [5]

$$Q(t)/Q_\infty = 2(D_E t/\pi l^2)^{1/2} \tag{15}$$

where $D_E=D$=const. for a system obeying Fick's law. On the other hand, D_E represents a rather complex "weighted mean" diffusivity in the range C_l to C_o for concentration dependent D. However, the average diffusivity for a complete absorption (D_E^a)–desorption (D_E^d) cycle approximates very closely the mean diffusivity determined from steady-state permeation (see eq. 13b) [5]

$$\bar{D} \cong \tfrac{1}{2}(D_E^a + D_E^d) \tag{16}$$

This is the most common sorption-based method for determining D=const. or $\bar{D}(C_o,C_l)$. In the latter case, a series of experiments is performed. A series of "interval" experiments, where $|a_o-a_1|$ is kept small and a_1 is varied, can yield $D(C)$ practically

directly. In a series of "integral" experiments, a_1 (usually zero for absorption experiments) is kept constant and a_o varied; $D(C)$ is then obtained by differentiation of eq. (13b) (see [5]).

Analogous series of permeation experiments may, of course, be used to study the behavior of $\overline{P}\,(C_o,C_l)$, $P(C)$.

(b) At sufficiently long times, for a system obeying Fick's law

$$Q(t)/Q_\infty = 1 - (8/\pi^2)\exp(-D_2\pi^2 t/4l^2) \qquad (17)$$

which yields a linear plot of $\ln[1-Q(t)/Q_\infty]$ vs t with $D_2=D$. For a concentration dependent system, the plot is non-linear but the long-time slope eventually approaches the value characteristic of $D_2=D(C_o)$ [5].

3.3 Fickian vs IRT formalism for the diffusivity of CCl_4 in mesoporous alumina

This system (studied in [6]) exhibits strong concentration-dependent deviations from Fick's and Henry's laws. It is characterized by what is known as a type IV sorption isotherm C vs a [7]. Because of the low vapor pressure of CCl_4, the vapor may be treated as an ideal gas. We thus set $a=a_R\cong p/RT=c_g$ (see Fig. 2a). The initial portion of this isotherm (which coincides with that of loose alumina powder) corresponds to the formation of a monolayer of adsorbed molecules on the surfaces of the pore walls (or of the grains of loose powder) and leads to increasing negative deviations from Henry's law, as the said monolayer is progressively densified. This tendency should ultimately lead to a plateau in the isotherm, as the monolayer approaches saturation, if it were not for the intervening initiation of a second layer of more weakly adsorbed molecules on top of the first. Liquidlike multilayers of CCl_4 adsorbate are thus readily built up (see Fig. 2b,c), as c_g is further increased. They are characterized by properties not very different from those of bulk liquid and lead to a steep rise of the isotherm for both powder and porous medium. In the latter case, a plateau is reached at the point where the pores become saturated with liquid sorbate. This plateau is attained sooner than might be expected on the basis of multilayer-thickness (t_s) growth, because of intervening condensation (due to capillary phenomena). Thus, a pore of radius r fills up with condensate at the point where the empty core radius ($r-t_s$) falls below a critical size r_K (known as the Kelvin radius) which is a function of p/p_{sat}. The occurrence of condensation in the porous medium is evidenced by the appearance of a characteristic absorption-desorption hysteresis loop, when c_g is progressively reduced back to zero [7]. This phenomenon (most probably due to the existence of filled pores in the interior of the porous medium, which are supercritical at a given p but are denied exposure to the external vapor phase by surrounding subcritical filled pores) does not appear to affect materially the concentration dependence of the diffusion behavior of interest here.

Strictly speaking, account should be taken of the fact that pore space not occupied by adsorbate contains occluded vapor, which can also contribute to the measured overall sorption S and permeability P coefficients. Denoting by C_g, C_s (in mol/cm^3 of porous medium) the concentrations of occluded vapor and of adsorbate, respectively, we find that, of the total porosity ε of the medium, the part occupied by adsorbate is $\varepsilon_s=V_LC_s$

(where V_L may be identified with liquid molar volume without serious error). Hence, $S_g=C_g/c_g=\varepsilon-\varepsilon_s$; which is generally negligible by comparison with $S_s=\varepsilon_s/V_L c_g$; i.e.

$$S_s = S - S_g \cong S \tag{18}$$

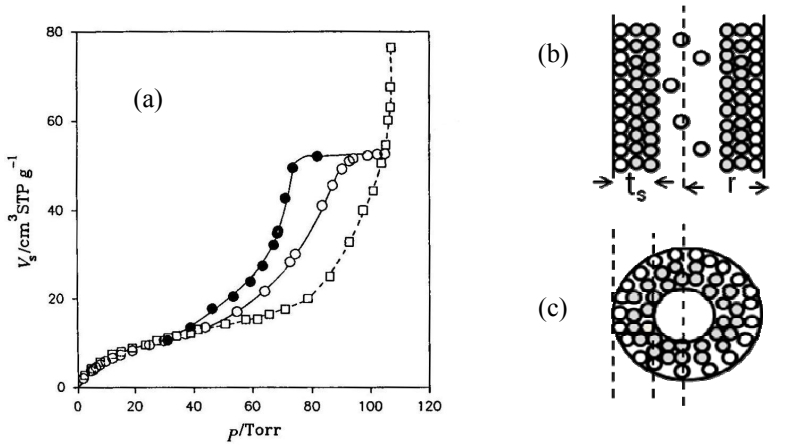

Fig. 2: (a) Sorption isotherm of CCl_4 by alumina porous septum (○, adsorption branch; ●, desorption branch) and loose powder (□) (amount of sorbate V_s vs vapor pressure p); from [6]. (b) Schematic representation of a cylindrical pore of radius r with multilayer of adsorbate of thickness t_s and occluded vapor molecules (side view). (c) Top view.

Similarly for the corresponding permeability coefficient we have

$$P_s \equiv S_s D_{Ts} = P - P_g = P - (\varepsilon - \varepsilon_s) D_{gT} \tag{19}$$

where $D_{Tg}\equiv D_g$=const. may be identified with the diffusivity for Knudsen flow and may thus be evaluated at any ε_s by measuring the permeability of He (assumed to be pure gas-phase) $P_{He}=(\varepsilon-\varepsilon_s)D_{He}$ and applying the following relation [8] (where M_g denotes gas molecular weight)

$$D_g = D_{He}(M_g/M_{He})^{1/2}$$

On this basis, and using $v_s=\varepsilon_s/\varepsilon$ as a convenient adsorbate concentration parameter, series of (concordant) "interval" and "integral" permeation experiments, covering the full range $v_s = 0 - 1$, were performed (as described in section 3.2). The data, when analysed (following previous practice for analogous systems, see e.g. [8-13]) in terms of the Fick formalism $D_s(v_s)=P_s(dx/dC_s)$ [see eq. (1a)], gave results (see Fig. 3) closely similar to those pertaining to the aforesaid analogous systems. In particular, $D_s= D_s^o$ =const. (Fick's law) in the region of $v_s\to 0$ (not visible in Fig. 3); D_s then tends to increase with rising v_s in the submonolayer region. Energetic non-homogeneity of the pore surfaces is a plausible physical explanation for this behavior, because stronger adsorption sites are filled first and penetrant molecules adsorbed at these sites are less mobile. However, when v_s increases just beyond the point of completion of a monolayer (indicated by BET theory), D_s begins to decline, passes through a minimum and then increases strongly and

continuously as $v_s \rightarrow 1$. This strong increase may plausibly be attributed to the onset of adsorbate-multilayer hydrodynamic flow (in keeping with evidence from comparison of D_s and corresponding tracer diffusion coefficients D_s^* in analogous systems, which show $D_s \approx D_s^*$ in the low, and $D_s > D_s^*$ in the high, v_s region [12]). However, the behavior of D_s, in the intermediate v_s region, is very difficult to reconcile with physical insight (cf. the comment of Gilliland et al [11]: *"when diffusion coefficients vary in such a manner with concentration, the utility of the concept of diffusivity, as it is normally defined, has been lost for correlating purposes"*). However, when allowance was made for the thermodynamic factor φ_T inherent in D_s according to the IRT approach [see eq. (6)], the mobility of adsorbate, represented by $D_{Ts}=P_s/S_s$ [see eq. (19)], was found (see Fig. 4; cf. also [14]) to increase smoothly from the submonolayer region up to the saturation of the porous medium with condensate (v_s=1) (in contrast to the behavior of D_s, which approaches v_s=1 tangentially; see Fig. 3). The resulting $D_{Ts}(v_s=1)=D_{TL}$ is related to the hydraulic permeability P_{HL}, usually defined for hydrodynamic flow, by $D_{TL} = RTP_{HL}/\varepsilon V_L$.

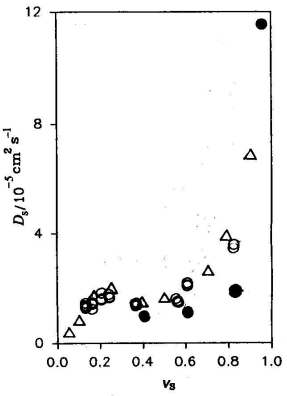

Fig. 3: Concentration dependence of the Fick adsorbate diffusivity D_s in terms of v_s (fraction of pore volume occupied by liquidlike sorbate); ○,△ absorption; ● desorption. From [6].

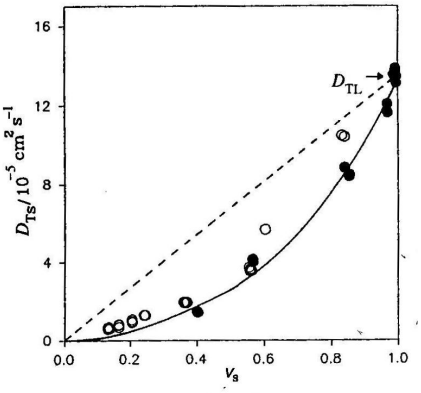

Fig. 4: Concentration dependence of the thermodynamic surface diffusivity D_{Ts} in terms of v_s, in comparison with the curve (——) predicted by eq. (20); - - - - model of [16]; symbols as in Fig. 3. From [6].

Furthermore the aforeseen experimental D_{Ts} behavior has received remarkable support from a simple new physical approach applicable to multilayer adsorbate flow, in a single cylindrical capillary [15]; which supersedes the previous analogous one of [16] and yields a more accurate prediction of the concentration dependence of D_{Ts}/D_{TL} (see Fig. 4) not subject to any external (or internal adjustable) parameters, namely

$$D_{Ts}/D_{TL} = 3v_s - 2 - (2/v_s)(1 - v_s)^2 \ln(1 - v_s) \qquad (20)$$

Physically, the experimental applicability of this relation is subject to (i) the limitations of simple multilayer adsorption theory (which obviously becomes increasingly inappropriate near, and even more so below, the monolayer region) and (ii) the effects of the structural complexity of real porous media and of simultaneous condensation. Fortunately, these

effects have been shown (by simulation based on sophisticated pore network models) to be relatively small [17] and eq. (20) was found [15] to provide a good fit to the data reported in [10] on CH_2Cl_2 diffusing in mesoporous silica.

4. Time Dependent Non-Fickian Diffusion (Relaxing Medium)

4.1 Theory

Polymer–organic vapor systems usually exhibit concentration-dependent diffusion behavior, with S a weak, and D_T a strong, function of the concentration of sorbed penetrant C (which is defined here in a *polymer-fixed* frame of reference, namely in moles per unit volume of penetrant-free polymer), due to penetrant-induced swelling and plasticization of the polymeric medium. For rubbery polymeric systems, characterized by high segmental mobility (glass transition temperature T_g of the system well below the experimental temperature T), the relevant swelling process is fast relative to diffusion and the resulting sorption kinetics is Fickian. For glassy polymeric systems (characterized by $T_g>T$), on the other hand, completion of the local swelling process may be sufficiently slow (*delayed swelling*) to exercise a substantial, and even controlling, influence on sorption rate and kinetics (with attention focused here primarily on absorption kinetics).

To model such non-Fickian sorption kinetics in a genuine Fickian spirit, recourse has to be made to a well-studied analogue of delayed swelling; notably the deformation of a viscoelastic solid under an applied mechanical stress. In the simplest practically useful approach of this kind, the (assumed linear) viscoelasticity of the solid is represented by a "mechanical equivalent" consisting of a Maxwell element (i.e. a spring of elastic modulus E_a in series with a dashpot of viscosity η_a) in parallel with a spring of elastic modulus E_b (see Fig. 5). Application of a constant stress σ_1 (creep experiment) produces an instantaneous (elastic) strain $e_1^o=\sigma_1/E^o$ ($E^o=E_a+E_b$ is the initial or instantaneous elastic modulus), which relaxes (due to viscous flow in the dashpot) to a final strain $e_1^\infty=\sigma_1/E^\infty$ ($E^\infty=E_b$ is the final or equilibrium elastic modulus). The general relation between the evolution of an applied stress and of the resulting strain, in this mechanical model system, is given by (e.g. [18])

$$de/dt = (1/E^o)(d\sigma/dt) + (E^\infty\beta_a/E^o)(e^\infty - e) \qquad (21)$$

where $\beta_a=E_a/\eta_a$ = viscous relaxation frequency (reciprocal relaxation time); $e^\infty=\sigma/E^\infty$.

Similarly, a non-Fickian polymer-vapor system may be characterized by a relaxation-dependent sorption coefficient S (which, for present modeling purposes, may be assumed,

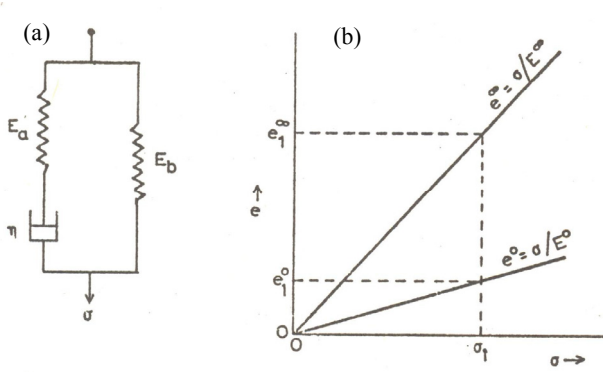

Fig. 5: (a) Mechanical equivalent model of linear viscoelastic behavior of a solid (b) Schematic stress (σ) – strain (*e*) relations at t=0 and t=∞ (see text).

without loss, to be concentration-independent). Under conditions of sorption fully controlled by viscous relaxation (cf. "second-stage" absorption below), S may vary, at a given activity $a=a_1$, from an initial value $S^o=C^o/a_1$ to a final value $S^\infty=C^\infty/a_1$ corresponding to $1/E^o$ and $1/E^\infty$ respectively. For a more exact analogy (using subscripts A and B, to distinguish between penetrant and polymer properties respectively, where necessary), we define a swelling strain $V_A dC$ (where V_A=liquid partial molar volume assumed constant) resulting from a (tensile) osmotic stress dπ applied on the polymer, given by

$$d\pi = -d\mu_B/V_B = (n_A/n_B V_B)d\mu_A \tag{22}$$

where V_B is polymer partial molar volume (assumed constant); n denotes number of moles; and the Gibbs-Duhem relation has been applied. Given the condition of thermodynamic equilibrium applied above, eq. (3) and the definition of C and S, we get finally

$$d\pi = C^\infty d\mu_A = (RTC^\infty/a)da = RTS^\infty da \tag{23}$$

Thus, given $S^\infty \approx$const. (v.s.), we may replace e in the ordinate of Fig. 5b by CV_A and σ in the abscissa by $\pi=RTS^\infty a$, with moduli $E^\infty=RT/V_A$ and $E^o=RTS^\infty/S^oV_A$. The lines for e^∞ and e^o in Fig. 5b now reduce to scaled versions of the sorption isotherms of C^o vs a and of C^∞ vs a respectively. These isotherms reflect, respectively, fast very local, and slow longer range, microstructural relaxations needed to accommodate incoming penetrant molecules (or to close gaps left behind by outgoing penetrant molecules in the case of desorption; which is not considered here in the interest of brevity). Hence, the counterpart of eq. (21) here is (after cancellation of V_A which appears on both sides)

$$\partial C/\partial t = S^o(\partial a/\partial t) + \beta(C^\infty - C) \tag{24}$$

where $\beta=\beta_a S^o/S^\infty=\beta_a E^\infty/E^o$ is an effective viscous relaxation frequency, analogous to a first-order rate constant in chemical kinetics, (but bearing in mind that β, like D_T, is here an exponential function of C). Eq. (24) must be solved simultaneously with the IRT diffusion equation obtained by substitution of eq. (4) in eq. (8)

$$\partial C/\partial t = (\partial/\partial x)[D_T S(\partial a/\partial x)] \tag{25}$$

under the boundary conditions imposed by eqs (14) (sorption) or (9) (permeation). In the latter case, the effect of relaxation is to delay attainment of the steady state and yield a time lag L^a exceeding the value L_s^a expected for a fully relaxed (Fickian) system [19,20].

On the other hand, absorption experiments yield a rather broad spectrum of kinetics, which has been studied extensively. The more straightforward kinetic features predicted by the above modeling approach [21] (for examples of other approaches, differing more or less significantly therefrom, see e.g. [22-27]) depend primarily on the behavior of the *kinetic modulus* $l^2\beta(C)/D_T(C)$ [22], which provides a measure of the rate of relaxation (governed by β) relative to that of diffusion (governed by D_T/l^2).

As indicated above, sorption experiments wherein $l^2\beta/D_T >> 1$ conform to the basic characteristics of Fickian kinetics, namely (i) initially linear $Q(t)$ vs $t^{1/2}$ plots and (ii) coincident $Q(t)/Q_\infty$ vs t/l^2 curves for different l. For $l^2\beta/D_T << 1$, a two-stage $Q(t)$ vs $t^{1/2}$ plot is predicted, representing fast diffusion through practically unrelaxed polymer (stage I) and viscous delayed swelling, not significantly complicated by diffusion (stage II), respectively. A study of stage II absorption kinetics of benzene in atactic polystyrene [28] gave results practically coincident with those obtained from parallel mechanical creep experiments, thus providing strong quantitative evidence of the close physical similarity of viscous swelling and mechanical relaxation processes.

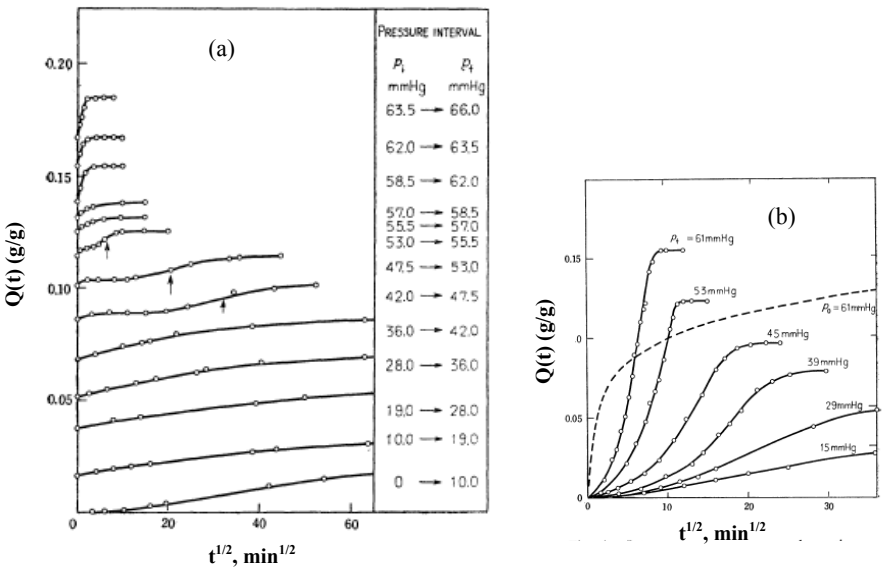

Fig. 6: Sorption kinetics of methyl ethyl ketone, under the given external initial and final vapor pressures, in atactic polystyrene. (a) Series of interval sorption runs. (b) Series of integral sorption runs and one desorption run (broken line). From [29].

As $l^2\beta/D_T$ assumes higher values, the said two stages tend to merge, yielding eventually a single S-shaped $Q(t)$ vs $t^{1/2}$ curve, with non-coincident $Q(t)/Q_\infty$ vs t/l^2 plots. Further increase of $l^2\beta/D_T$ ultimately leads, of course, to Fickian kinetics, as already noted above.

Such transitions from two-stage, to ultimately Fickian, kinetics are commonly seen in the high concentration range of series of interval absorption runs (where the initial activity a_1 is raised from one experiment to the next in relatively small steps; see section 3.2), as shown in the upper part of Fig. 6a [29]. On the basis of the above model predictions, such behavior is attributable to strong (positive) concentration dependence of the modulus $l^2\beta(C)/D_T(C)$. This interpretation ties up with the fact that increasing penetrant-induced plasticization of the polymeric medium, caused by rising C, past the point of transition to the rubbery state (as evidenced by the appearance of Fickian kinetics), is accompanied by strong concentration dependence of β (which rises effectively to infinity in the rubbery state) far exceeding that of D_T. On the other hand, the occurrence of S-shaped $Q(t)$ vs $t^{1/2}$ (changing to so-called "pseudo-Fickian") curves in the lower concentration (glassy) range (lower part of Fig. 6a) is attributable to the effect of differential swelling stresses [30], generated by (and decaying with) concentration gradients (in close analogy to the well known thermal stresses generated by temperature gradients); which need not concern us here.

In series of integral absorption runs, with starting point $a_1=C_1=0$ for each run (see section 3.2), only S-shaped $Q(t)$ vs $t^{1/2}$ plots are normally obtained for all final $C_o=S^{\infty}a_o$, as illustrated in Fig. 6b [29]. However, replots of the high-C_o curves (which usually extend to the rubbery state) reveal, in some systems studied (see example in Fig. 7), a new kinetic feature, namely a linear $Q(t)$ curve (zero-order sorption kinetics, allowing for some initial induction period), often referred to as *C*ase II diffusion. This process is associated with a flat high-concentration profile (C vs x) ending at a sharp penetration front, the low-concentration part of which extends to form a diffuse "precursor front" (assumed to obey Fick's law), as illustrated in Fig. 8. The whole concentration profile remains practically unchanged, as it propagates within the space $0 \le x \le l$, under semi-infinite medium conditions, with constant velocity v_o.

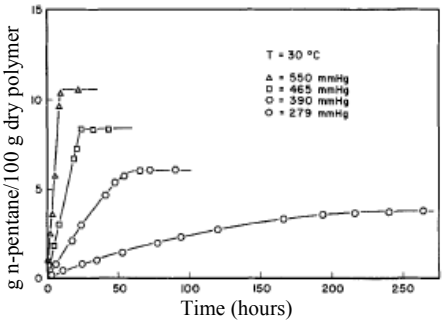

Fig. 7: Series of integral absorption runs, plotted on a t scale, for biaxially oriented polystyrene-n pentane. From [31].

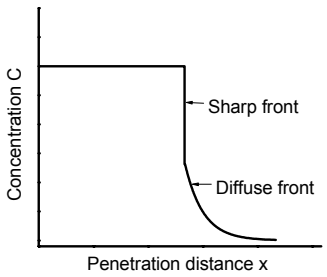

Fig. 8: Schematic Case II penetration profile as normally perceived (perfectly sharp propagating front preceded by a Fickian diffuse front).

This seemingly simple, but obscure, absorption kinetics was originally studied by postulating the presence of a constant-velocity convection term [23]. The function of a physically meaningful approach is, of course, to predict both the formation and mode of

propagation of the Case II profile, in the first place. Substantial progress in this direction, was made, invoking the mechanical analogy, e.g. in [32] and especially in [33], where extensive physically predictive model computations of Case II kinetics are reported, but the model used cannot account for some typical interval sorption kinetics noted above.

In terms of the more widely applicable (v.s.) modeling approach presented here [21] (for other similar approaches, see e.g. [24, 26, 27]), the physical basis of Case II kinetics may be outlined as follows:

(a) Relaxation kinetics

For convenience, the shorthand notation $D_{To}=D_T(C=0)$, $D_{TF}=D_T(C=C_o^\infty)$, $\beta_o=\beta(C=0)$, $\beta_F=\beta(C=C_o^\infty)$, is used. The relaxation expression introduced in eq. (24), rewritten as

$$\partial C/\partial t = \beta_o \exp(k_B C)(C^\infty - C) \tag{26}$$

with k_B=const., $C(t=0)=C^o$, $C(t\rightarrow\infty)=C^\infty$, and under conditions of $\beta_F>>\beta_o$, $C^\infty>>C^o$, yields solutions $C(t)$, which rise slowly at first but become very steep as $C\rightarrow C^\infty$ (see example for $C^o=0$, $\beta_F/\beta_o=10^4$ in Fig. 9 [34]). This behavior closely parallels "delayed yielding" kinetics in mechanical creep experiments (illustrated in Fig. 10 [35]). The "swelling yield" feature is associated with an inflection point in C(t) (designated by $C=C_R$), which appears if the condition $k_B(C^\infty-C^o)>1$ is satisfied. The corresponding time $t(C=C_R)=t_R$ affords a useful measure of the effective lifetime of a relaxation process of the type envisaged here.

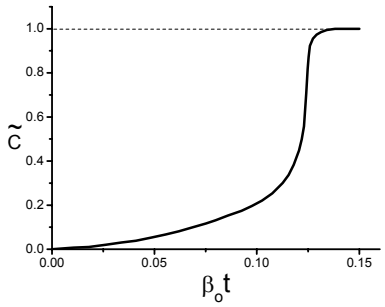

Fig. 9: Example of a solution of the relaxation equation (26); $\tilde{C}=C(t)/C^\infty$, ($C^o=0$ and $\beta_F/\beta_o=10^4$) exhibiting a final steep rise to $C(t)=C^\infty$ (with inflection point at $C_R=0.89C^\infty$). From [34].

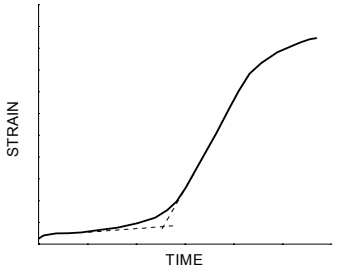

Fig. 10: Schematic illustration of mechanical creep curve exhibiting delayed yielding. Adapted from [35].

(b) Behavior of the kinetic moduli

The basic conditions for Case II kinetics, in the space $0\leq x\leq l$, are given as

$$l^2\beta_o/D_{To} \geq 1\ ;\quad l^2\beta_F/D_{TF} >> 1\ ;\quad l^2\beta_o/D_{TF} << 1 \tag{27a,b,c}$$

Conditions (27a) and (27b) involve the kinetic modulus defined previously. The former represents diffusion in a relatively slowly relaxing (glassy) polymeric medium

(where the precursor front tends to shrink, as the value of this modulus rises). The latter condition represents Fickian diffusion in the relaxed (rubbery) swollen polymer. Finally, condition (27c) defines a new kinetic modulus, which ensures that the overall penetration process is rate-controlled by slow viscous relaxation in the low-concentration (glassy) region.

Fig. 11 presents an early example of the results obtained by simultaneous solution of eqs (24) and (25), representative of the diffusion and viscous relaxation conditions stated above [21]. The generation of the penetration front may be understood in terms of the $C(t)$ kinetic results derived from eq. (26), which are directly applicable to the exposed surface (x=0) of the polymer film, if we put $C^{\infty}=C_o^{\infty}=S^{\infty}a_o$ and $C^{o}=C_o^{o}=S^{o}a_o$. The induction period in Fig. 11a is obviously attributable to the pre-yield slow relaxation of $C_o(t)$, which is still going on at stage (A), as is confirmed by the associated (purely precursor) concentration profile in Fig. 11b.

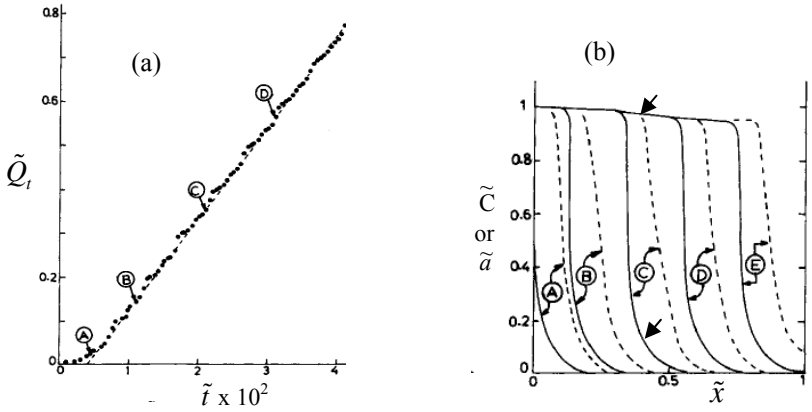

Fig. 11: (a) Computed plots of $\tilde{Q}_t=Q(t)/Q_{\infty}$ vs $\tilde{t}=D_o t/l^2$ for a model integral absorption run with $l^2\beta_o/D_o$=10, $l^2\beta_F/D_F$=20, $l^2\beta_o/\beta D_F$=0.02. (b) Associated profiles of concentration $\tilde{C}=C/C_o^{\infty}$ (——) or activity $\tilde{a}=a/a_o$ (- - - -) vs $\tilde{x}=x/l$. From [21].

Fig. 11a shows that, after completion of the relaxation process at x=0 ($C_o=C_o^{\infty}$), good conformity (within the limits of available computer resources) to Case II kinetics is observed; while the corresponding penetration fronts (B, C, D, E) in Fig. 11b (full lines) duly conform to the pattern shown in Fig. 8 and remain reasonably constant in time. Further studies have shown that the velocity of propagation v_o is very highly correlated to t_R.

To gain better understanding of the mechanism underlying the above results, note that the steep part of the penetration front reflects viscous swelling kinetics in the yield region (as can be shown by introducing $J=v_oC$ in eq. (8) to obtain $\partial C/\partial t=-v_o\partial C/\partial x$). The constancy of v_o requires constancy of t_R. This is achieved thanks to the very flat high-activity $a(x,t)\cong a_o$ profiles (see broken lines in Fig. 11b), which propagate well ahead of the corresponding concentration profiles $C(x,t)$. The crucial result is that, at any x, $a(x,t)\cong a_o$ is attained while the relaxation of $C(x)$ is still at the pre-yield stage. [This is

illustrated for stage C in Fig. 11b, where the attainment of $a(x) \cong a_o$ is marked by arrows on the corresponding activity and concentration profiles]. Accordingly, swelling yield, at *all* x, occurs, under the *same* boundary condition $C(x) \approx C_o^{\infty} = S^{\infty} a_o$ [34], thus yielding t_R=const.

4.2 Practical example

To illustrate the practical applicability of this modeling approach, we consider the example of bidimensional diffusion of liquid swelling agents into uniaxially oriented cellulose acetate films (containing 2.45 acetate groups per monomer unit), sandwiched between clamped glass plates to allow penetration only across the exposed edges of the films (see Fig. 12). Microscopic observation at right angles to the plates showed inward-moving penetration fronts and corresponding outward-moving swelling fronts. Penetration rate (as well as swelling rate) was relatively fast and obeyed Fickian kinetics

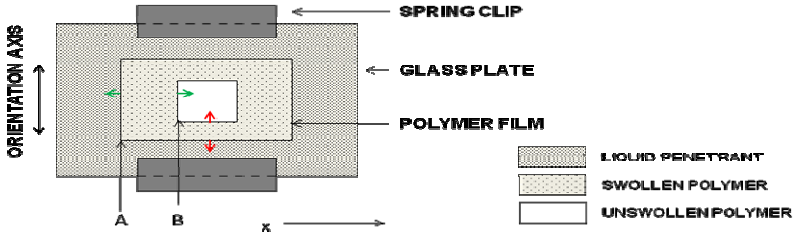

Fig. 12: Top view of schematic presentation of experimental setup for bidimensional penetration of liquid CH_2Cl_2 in uniaxially oriented cellulose acetate [36, 37]. A: swelling front; B: penetration front.

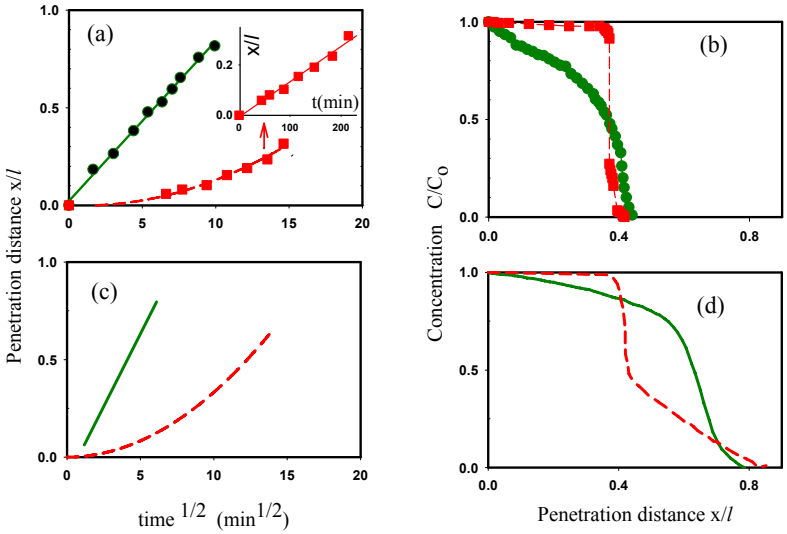

Fig. 13: (a) Experimental penetration curves (b) Experimental concentration profiles (c) simulated penetration curves (d) simulated concentration profiles. Penetration normal (●, ——) or parallel (■, - - - -) to the axis of macromolecular orientation. From [36, 37].

normal to the axis of preferred molecular orientation, but was markedly slower and followed Case II kinetics *parallel* to the said axis, under otherwise identical conditions (see Fig. 13a). Microdensitometry [36] and microinterferometry [37] revealed typical concentration-dependent Fickian and Case II concentration profiles respectively (see Fig. 13b). Delayed swelling, in the present set up, arises from the constraint imposed by the clamping pressure on swelling of the film in the direction of the thickness. This constraint is relieved (and full volume swelling recovered) by longitudinal viscous swelling, which is fast (slow) in the direction normal (parallel) to the axis of preferred molecular orientation, in accord with the direction of easier (more difficult) deformability of the polymeric medium. The basic characteristics of this kinetic behavior have been successfully simulated (see Figs 13c-d [36]; computation for simulation of the precursor front as well, was too onerous to envisage at the time) by setting, for penetration parallel to the axis of molecular orientation: $l^2\beta_o/D_{To}=1$, $l^2\beta_F/D_{TF}=200$, $l^2\beta_o/D_{TF}=0.002$, $S^o/S^\infty=0.36$. Then, penetration normal to the said axis of orientation was simulated simply by increasing β_o by a factor of 10^3 (yielding new values of $l^2\beta_o/D_{To}=10^3$, $l^2\beta_o/D_{TF}=2$), keeping all other parameters the same.

5. Space-Dependent Non-Fickian Diffusion (Axially Inhomogeneous Medium)

5.1 Theory

We consider unidimensional diffusion (assuming for simplicity concentration-independent S and D_T) in the space $0\leq x\leq l$; wherein the solid medium exhibits variability

of some salient macroscopic structural characteristic (such as density or porosity), which translates to a functional dependence of S and D_T on x. Under these conditions, the equilibrium sorption and steady-state permeation measurements, referred to in section 3.2, yield effective sorption (S_e) and permeability (P_e) coefficients, which are averages (arithmetic or harmonic respectively) of $S(x)$ and $P(x)$, and an effective diffusion coefficient $D_e=P_e/S_e$ [38-42]. The latter relation is consistent with Fick's law, but the measured time lag L^a generally deviates from the expected value $L_s^a=l^2/6D_e$ [see eq. (12c)]. This result is a useful indicator of non-Fickian diffusion, but not of its physical nature, in view of the fact that such discrepancies are also expected in the case of time-dependent non-Fickian diffusion (see section 4). Note similar difficulties for the physical interpretation of absorption kinetics; for example, an S-shaped $Q(t)$ vs $t^{1/2}$ plot (see section 4) may also result from diffusion into a membrane with a surface "skin" of higher density (a common artefact of polymer film manufacture) and hence of lower S and D_T.

Valuable additional information in this respect is obtainable by extension of the standard method of permeation time-lag measurement, based on the initial condition $a(x,t=0)=a_l$ [see eq. (9a)], described in section 3.2. The extended method involves [38-42]: (a) measurement of the amount (per unit membrane area) of penetrant entering the membrane at $x=0$, $Q(0,t)$, in addition to the standard measurement of $Q(l,t)$ and (b) repetition of these measurements, under a "desorptive" initial condition $a(x,t=0)=a_o$ (in this case the experiment is started by dropping the activity at $x=l$ from $a=a_o$, to $a=a_l$). These measured "absorptive" (superscript a) and "desorptive" (superscript d) permeation curves (illustrated in Fig. 14) yield four time lags, namely $L^a(l)>0$, $L^a(0)<0$, $L^d(l)<0$, $L^d(0)>0$; which may, for convenience, be put in the form: $L^a \equiv L^a(l)$; $\Delta L^a=L^a-L^a(0)$; $\delta L=L^a-L^d(l)$; $\delta\Delta L=\Delta L^a-L^d(l)+L^d(0)$; for comparison with the corresponding time-lag parameters (denoted by subscript s) calculated for a system obeying Fick's law, with $S=S_e$ and $D=D_e$, given below

$$6L_s^a = 2\Delta L_s^a = 2\delta L_s = \delta\Delta L_s = \delta\Delta L = l^2/D_e$$

N.B. the above relation $\delta\Delta L=\delta\Delta L_s$; which enables determination of $S_e=P_e/D_e=P_e\delta\Delta L/l^2$ directly from permeation data, as was the case with Fick's law in section 3.2.

Study of the discrepancies between actual and calculated values of the other time-lag parameters, $L_E^a=L^a-L_s^a$ etc., reveals distinctive properties enabling clear discrimination between (as well as characterization of) time-dependent and space-dependent non-Fickian diffusion (the pertinent time lag discrepancies are designated as L_T^a etc., and L_h^a etc., respectively). If the said non-Fickian processes happen to coexist, the resulting discrepancies (at least in the simplest case under consideration here) are additive, i.e.,

$$L^a - L_s^a = L_T^a + L_h^a; \quad \Delta L^a - \Delta L_s^a = \Delta L_T^a + \Delta L_h^a; \quad \delta L - \delta L_s = \delta L_T + \delta L_h \qquad (28a,b,c)$$

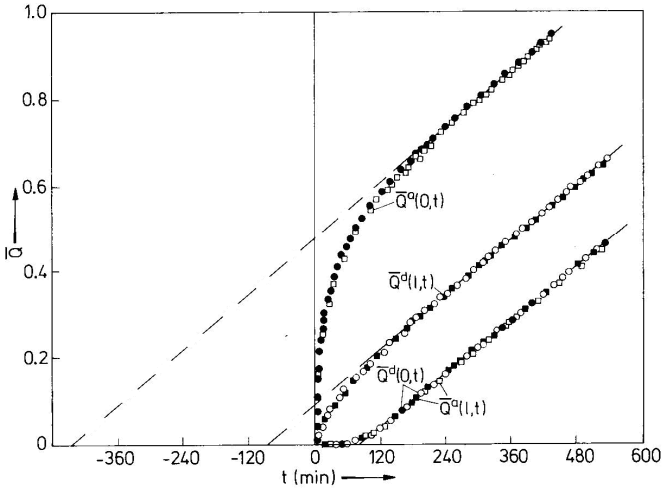

Fig.14: Experimental normalized absorptive (●, □) and desorptive (○, ■) permeation curves for N_2 diffusing in an unsymmetrically compacted graphite porous septum at 297K. From [42].

Thus, one may take advantage of the *general* properties: $\Delta L^a_T=0$ and $\Delta L^a_h=-\delta L_h$; to extract the values of ΔL^a_h and δL_T from eqs (28b,c) and thus obtain evidence regarding the presence (and, to some degree, the character) of each one of the coexisting non-Fickian processes.

General space-dependent time-lag behavior is, in effect, governed by the "transport function" $\psi(x)\equiv S(x)P(x)/S_eP_e$ and it is found that the algebraic sign and magnitude of L^a_h and $\Delta L^a_h=-\delta L_h$ can serve as useful diagnostics of the functional form of $\psi(x)$ and of the relative degree of inhomogeneity [38-42]. Thus, $\Delta L^a_h=0$ is characteristic of a $\psi(x)$ symmetrical about the midplane of the membrane, with $L^a_h>0$ or $L^a_h<0$, if the turning point is a maximum or a minimum respectively; whereas $L^a_h<0$ with $\Delta L^a_h<0$ or $\Delta L^a_h>0$ imply unsymmetrical $\psi(x)$, with a preponderant tendency to increase or decrease with rising x respectively. Given an appropriate physical structure-property model, one may work back to the character of the underlying structural inhomogeneity of the medium.

5.2 Practical example

As an example, consider dilute gas (Knudsen) diffusion (obeying Fick's and Henry's laws) across a mesoporous septum (consisting of compacted powder) with diffusivities $D_{Tg}\equiv D_g$ and $D_{Ts}\equiv D_s$ for gas-phase and adsorbate flow respectively. We have [39-42]:

$$S = S_g + S_s = \varepsilon + A_o k_s(1-\varepsilon)\ ; \quad P = P_g + P_s = B_g\varepsilon^2/(1-\varepsilon) + A_o k_s(1-\varepsilon)D_s \qquad (29a,b)$$

where $A_o(1-\varepsilon)$ is the specific pore surface area (available for adsorption) per unit septum volume; k_s is the adsorption coefficient (strongly dependent on gas molecular weight M_g);

$B_g \approx$ const. (weakly dependent on M_g); A_o, B_g and k_s are effectively independent of x; but ε is a function of x, if the degree of compaction is not uniform across the septum.

In the case of helium, $k_s \approx 0$; hence the expected trend of $\varepsilon(x)$ is obviously the same as that of $\psi(x)$. Thus, according to what has been said above, the data of Table 1 (taken from [39-41]) lead to the conclusion (confirmed by direct measurements of local porosity [39], [41]) that symmetrical compaction (see G1) results in very nearly symmetrical $\varepsilon(x)$ with a minimum at $x=l/2$; whereas unsymmetrical compaction (under the conditions used in [39-41]) yields unsymmetrical $\varepsilon(x)$ with preponderant tendency to increase with increasing x (see C1, G2-G4). On the other hand, the magnitude of the normalized experimental ΔL_h^a of Table 1 shows that greater homogeneity of porosity is achieved by compaction in several small steps (cf. G2, G3) or to a lower overall porosity (cf. G3, G4). Table 2 verifies the prediction of the model of eq. (29) that, for sufficiently high k_s, the adsorbate term in eqs (29a,b) becomes dominant: this leads to $\psi(x)$ varying inversely with $\varepsilon(x)$. Accordingly, the negative experimental L_h^a values for the light gases [characteristic of a minimum in the corresponding $\psi(x)$] become positive for the heavier gases [characteristic of a maximum in $\psi(x)$].

Table 1. Time-lag parameters for He diffusing in activated-carbon (C1) or graphite (G1-G4) porous septa of porosity ε prepared by symmetrical or unsymmetrical powder compaction in 1-12 steps.

Porous medium	ε	L_h^a / L_s^a	$\Delta L_h^a / \Delta L_s^a$
C1 unsym (12)	0.50	-0.14	0.16
G1 sym (1)	0.15	-0.15	-0.05
G2 unsym (1)	0.15	-0.38	0.42
G3 unsym (5)	0.13	-0.35	0.16
G4 unsym (6)	0.24	-0.58	0.62

Table 2. Time-lag parameters for a series of gases of increasing adsorbability (k_s) diffusing in a symmetrically compacted graphite septum of porosity 0.30 [43].

Gas	k_s/nm	L^a/min	L_h^a/min
He	–	3.2	-0.3_3
Ne	0.2	7.6	-0.6
Ar	4.6	25.3	-0.8_5
CH_4	15.1	37.2	0.8
Kr	16.8	90.0	1.2

6. Conclusion

The primary objective of the present paper is to familiarize a wider audience with (not to provide a full-fledged review of) the formulation and physical modeling of diffusion of a penetrant in a solid medium, exhibiting kinetic behavior more complicated than could be expected on the basis of the analogy of Fick's law with those of Fourier and Ohm.

The question is how far can Fick's formalism be taken to deal satisfactorily with complications due to (i) concentration dependence (ii) time dependence or (iii) space (x) dependence of the transport parameters. The answer is "not very far":

Formulation of case (i) in terms of $D(C)$ is viable mathematically but physically the Fick formalism is inferior to the IRT one and may even prove misleading in extreme (but in practice not uncommon) situations (as shown in section 3.3). In case (ii), time dependence could be introduced into the Fick formalism only through the surface boundary condition $C_o(t)$ [4], which *ab initio* could not possibly account for the

occurrence of relaxation in the *body* of the polymeric medium [20, 21]. Finally, formulation of x-dependence in terms of $D(x)$ [44], is clearly inadequate, as it obviously ignores the effect of $S(x)$ shown in section 5 to be particularly important. Thus, both of the last two cases can only be dealt with adequately by means of the IRT approach.

Fick's lasting achievement was to put basic material transport under the theoretical umbrella already put up for thermal and electrical transfer. This is, indeed, how science progresses ("*The specific of the senses, the generic of reason….without reason it is not possible to have science",* Aristotle). It is up to us to deal with the many more ramifications of material transport (Fourier or Ohm had to deal with only one kind of thermal or electrical fluid) in the same spirit.

References

[1] A. Fick, The London, Edinburgh and Dublin Philosophical Magazine and Journal of Science, 10 (1855) 30-39 (English abstracted version).
[2] J. W. Gibbs, The Collected Works of J. Willard Gibbs, Yale University Press, New Haven, 1948, Vol. 1, pp.429-430.
[3] J. Kaerger, D. M. Ruthven, Diffusion in Zeolites, Wiley, New York, 1992, Chap. 3.
[4] H. Fujita, Fortschr. Hochpolymer Forsch. 3 (1961) 1.
[5] J. Crank, Mathematics of Diffusion, Oxford University Press, 2nd ed., 1975.
[6] J. H. Petropoulos, G. K. Papadopoulos, J. Chem. Soc., Faraday Trans. 92 (1996) 3217.
[7] S. J. Gregg, K. S. W. Sing, Adsorption, Surface Area and Porosity, Academic Press, New York, 2nd ed., 1982.
[8] R. M. Barrer in E. A. Flood (Ed.), The Solid-Gas Interface, Marcel Dekker, New York, 1967, vol. 2, chap. 19.
[9] P. C. Carman, F. Raal, Proc. R. Soc., London, Ser. A, 209 (1951) 38
[10] P. C. Carman, Proc. R. Soc., London, Ser. A, 211 (1952) 526.
[11] E. R. Gilliland, R. F. Baddour, J. L. Russell, AIChE J. 4 (1958) 90.
[12] M. Okazaki, H. Tamon, T. Hyodo, R. Toei, AIChE J. 27 (1981) 1035.
[13] Y. D. Chen, R. T. Yang, AIChE J. 39 (1993) 599.
[14] P. Rajniak, R. T. Yang, AIChE J. 42 (1996) 319.
[15] J. H. Petropoulos, Langmuir, 12 (1996) 4814.
[16] M. E. Huber, E. A. Flood, R. D. Heyding, Can. J. Chem. 34 (1956) 1288.
[17] J. H. Petropoulos, G. K. Papadopoulos, Langmuir 23 (2007) 12932-12936.
[18] R. G. C. Arridge, Mechanics of Polymers, Clarendon Press, Oxford, 1975, p. 57.
[19] A. Kishimoto, J. Polym. Sci., Part A, 2 (1964) 1421
[20] J. H. Petropoulos, P. P. Roussis, J. Chem. Phys. 47 (1967) 1491.
[21] J. H. Petropoulos, J. Polym. Sci., Part B, 22 (1984) 1885.
[22] J. Crank, J. Polym. Sci. 11 (1953) 151.
[23] H. B. Hopfenberg, V. Stannett in: R. N. Haward (Ed.), The Physics of Glassy Polymers, Applied Science Publ., London, 1973, Chap. 9.
[24] C. J. Durning, J. Polym. Sci., Part B 23 (1985) 1831.
[25] J. H. Petropoulos, J. Polym. Sci., Part B, 22 (1984) 183.
[26] J. C. Wu, N. A. Peppas, J. Polym. Sci., Part B, 31 (1993) 1503.
[27] G. Camera-Roda, G. C. Sarti, AIChE J. 36 (1990) 851.

[28] M. Tamura, K. Yamada, H. Odani, Rep. Progr. Polym. Phys. Japan 6 (1963) 163.
[29] H. Odani, J. Hayashi, M. Tamura, Bull. Chem. Soc. Japan 34 (1961) 817.
[30] M. Sanopoulou, P. P. Roussis, J. H. Petropoulos, J. Polym. Sci., Part B, 33 (1995) 993.
[31] H. B. Hopfenberg, R. H. Holley, V. Stannett, Polym. Eng. Sci. 9 (1969) 242.
[32] G. C. Sarti, Polymer 20 (1979) 827.
[33] N. L. Thomas, A. H. Windle, Polymer 23 (1982) 529.
[34] M. Sanopoulou, D. F. Stamatialis, J. H. Petropoulos, Macromolecules 35 (2002) 1012.
[35] D. H. Ender, J. Appl. Phys. 39 (1968) 4877.
[36] J. H. Petropoulos, M. Sanopoulou, J. Polym. Sci, Part B, 26 (1988) 1087.
[37] M. Sanopoulou, J. H. Petropoulos, J. Polym. Sci, Part B, 30 (1992) 983.
[38] J. H. Petropoulos, P. P. Roussis, J. Chem. Phys., 47 (1967) 1496.
[39] C. Savvakis, J. H. Petropoulos, J. Phys. Chem., 86 (1982) 5128.
[40] P. Galiatsatou, N. K. Kanellopoulos, J. H. Petropoulos, J. Membr. Sci. 280 (2006) 634.
[41] P. Galiatsatou, N. K. Kanellopoulos, J. H. Petropoulos, Phys. Chem. Chem. Phys., 8 (2006) 3741.
[42] J. H. Petropoulos, Adv. Polym. Sci. 64 (1985) 93.
[43] J. H. Petropoulos, V. Havredaki, J. Chem. Soc., Faraday Trans. 1, 82 (1986) 66.
[44] R. Ash, R. W. Baker, R. M. Barrer, Proc. R. Soc, London, Ser. A, 304 (1968) 407.